Body Surface Potential Propagation Maps During Macroreentrant Atrial Arrhythmias. A Simulation Study

Alejandro Liberos[1], Jorge Pedrón-Torrecilla[1], Miguel Rodrigo[1], José Millet[1], Andreu M Climent[2], María S Guillem[1]

[1]Bio-ITACA, Universitat Politècnica de València, Valencia, Spain
[2]Hospital General Universitario Gregorio Marañón, Madrid, Spain

Abstract

Atrial flutter (AFL) is a supraventricular arrhythmia perpetuated by a macroreentrant circuit around an obstacle. Typical AFL is caused by a rotation around the tricuspid annulus (TA) and atypical AFL by a rotation around any other structure. The identification of the circuit in atypical AFL is complicated both by using the standard electrocardiogram and by the use of intracardiac recordings. In this work, we present mathematical simulations describing several macroreentrant behaviors in an atrial structure and its reflection on the torso. Specifically, we will discuss in detail a clockwise typical flutter and two atypical flutters dependent on inferior and superior vena cava respectively. We will also describe the detection and tracking of phase singularities and phase maps as a tool to summarize BSPM recordings.

This work presents the simulation of arrhythmic behaviors on realistic multicellular models and calculation of its reflection on the surface of the torso as a promising tool for verifying diagnosis techniques based on BSPM.

1. Introduction

Atrial flutter (AFL) is a supraventricular arrhythmia characterized by the presence in the electrocardiogram (ECG) of atrial complexes with constant morphology at a rate of 250-300 beats per minute. Although AFL is not a lethal arrhythmia it affects the quality of life of patients because of the effect of these rapid activations on the ventricular response [1]. Mechanism of perpetuation of AFL is a macroreentrant circuit or a circular activation around an obstacle. Depending on the structure that defines the reentrant circuit, AFL is subdivided into two categories: typical AFL, caused by a rotation around the tricuspid annulus (TA) and atypical AFL caused by a rotation around any other structure [2].

AFL can be terminated by ablation of some segment of the reentrant circuit, preferentially the narrowest portion of the circuit [3]. While in typical AFL this is almost a routine procedure, at which ablation involves breaking the conduction through the cavotricuspid isthmus, identification of the ablation target in atypical AFL is complicated both by using the standard electrocardiogram and by the use of intracardiac recordings. Localization of the circuit responsible of the reentrance prior to the ablation procedure may help in planning the intervention and thus reducing intervention times and improving success rates.

A non-invasive reconstruction of the atrial activation sequence based on the recording of multiple simultaneous ECGs may achieve this objective. Body Surface Potential Mapping (BSPM) has been successfully used for the non-invasive determination of spatial characteristics not obvious in the standard ECG. BSPM has been used for the localization of accessory pathways in Wolf-Parkinson-White [4], atrial fibrillation [5] and also in the discrimination of the direction of rotation in typical AFL patients [6, 7]. However, interpretation of BSPM maps is not trivial and this has prevented the introduction of this technique in the clinical setting. In this work, we present mathematical simulations describing several macroreentrant behaviors and their reflection on the torso as a new tool for the interpretation of BSPM maps during typical and atypical flutter. Specifically, we will discuss in detail a clockwise typical flutter and two atypical flutters dependent on inferior and superior vena cava (IVC and SVC) respectively. We will also describe the detection and tracking of phase singularities and the results obtained will be compared with a simulation of sinus rhythm.

2. Methods

2.1. Obtaining transmembrane potentials

Atrial activity was calculated by using an anatomically realistic atrial structure based in [8], consisting of 286174 nodes and with size 12.5x9 cm. The action potential of

each node was simulated by using Courtemanche mathematical model [9] which includes ionic currents, pumps and exchangers, and processes regulating intracellular concentration changes of Na^+, K^+ and Ca^{2+}. The model incorporated an extra potassium current, the acetylcholine (ACh) potassium current (I_{KACh}) [10]. This current produces a shortening in the action potential which favors the occurrence of arrhythmic behavior. The whole tissue is described as a monodomain model, after discretization of the spatial derivatives for an isotropic medium, the voltage evolution of the transmembrane voltage of each cell (i.e. V_i for the i-th cell), was controlled by the following first-order, time-dependent ordinary differential equation:

$$\frac{dV_i}{dt} = \frac{I_{total,i}}{C_m} - D\sum_j \frac{V_i - V_j}{d_{i,j}^2} \quad (1)$$

where D describes the diffusion of voltage through the medium, $I_{total,i}$ summarizes the contribution of all transmembrane currents [9], C_m is the transmembrane capacitance, and $d_{i,j}$ is the distance between neighbor cells i and j.

We adjusted D to obtain velocities of 100 cm/s for the bachman bundle and crista terminalis, 30 cm/s for the cavotricuspid isthmus and 60 cm/s for the rest of the atria, resulting in a full propagation of 99 ms.

Mathematical computations were performed on a system equipped with a Graphical Processing Unit NVIDIA Tesla C2075 6G based in Fermi and CUDA 4.0 by using an adaptive time-step solver based in Runge-Kutta [11].

We ensured a front propagation around the tricuspid annulus (TA) to simulate the clockwise typical FLA. To simulate atypical FLAs we forced a macroreentry around the obstacles desired (i.e. IVC and SVC). To achieve the occurrence of reentrant activity, D was reduced by 30%.

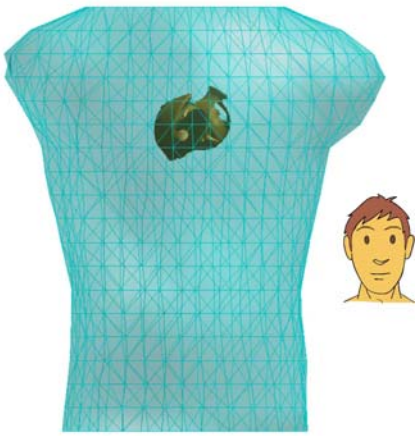

Figure 1: Torso model with 771 nodes and 1538 faces and atria model with 5988 nodes and 10680 faces.

We also simulated a sinus rhythm by stimulating the sinus node at a frequency of 75 bpm, with current pulses of 5nA and 5ms. In this case the effect of I_{KACh} was disabled.

2.2. Forward problem resolution

Simulated electrograms (EGMs) (i.e. 5988 signals) were calculated by using the transmembrane potentials generated:

$$EGM = \sum_{\vec{r}} \left(\frac{\vec{r}}{r^3} \right) \cdot \vec{\nabla} V_m \quad (2)$$

where $\vec{r}$ is the distance vector between the measuring point and a point in the tissue domain (r is the euclidean distance -1mm-), $\vec{\nabla}$ denotes the gradient operator and V_m is the transmembrane potential.

According to the BEM formulation [12-14], potentials on the surface of the torso can be computed from potentials on the heart surface by using (3)-(5):

$$A_1 x = b \quad (3)$$

$$A_1 = \begin{pmatrix} D_{HH(nxn)} & G_{HH(nxn)} \\ D_{TH(mxn)} & G_{TH(mxn)} \end{pmatrix}, \quad x = \begin{pmatrix} \Phi_H \\ \Gamma_H \end{pmatrix}, \quad b = \begin{pmatrix} -D_{HT(nxm)}\Phi_T \\ -D_{TT(mxm)}\Phi_T \end{pmatrix} \quad (4)$$

$$\Phi_T = A\Phi_H = \left(D_{TT} - G_{TH}G_{HH}^{-1}D_{HT}\right)^{-1} \cdot \left(G_{TH}G_{HH}^{-1}D_{HH} - D_{TH}\right)\Phi_H \quad (5)$$

where Φ_H is the potential on the surface of the heart, Φ_T is the potential on the surface of the torso, Γ_H is the potential gradient of the heart, D_{XY} is the potential transfer matrix from point Y to point X and G_{XY} is the potential gradient transfer matrix from point Y to point X.

Specifically, ECGs on a realistic torso model with 771 nodes and 1538 faces (Figure 1) were estimated. The ECG signals obtained were band-pass filtered from 2 to 10 Hz and represented in a plane.

2.3. Phase maps

Phase maps in the torso layer were obtained from the ECG phase signal of each node by using (6):

$$PS = \angle(HT(EG)) \quad (6)$$

where $\angle()$ is the phase operator and $HT()$ is the Hilbert Transform. The phase signal ranges from -π to π and represents the relative delay of each signal in one period.

2.4. Phase singularity definition and detection

A phase singularity (PS) was defined as the point in a phase map which is surrounded by phases from 0 to 2π. The phase value was obtained in 3 circles around each evaluated point, with radii of 0.06·Y, 0.12·Y and 0.2·Y, where Y was the height of the torso. A point was defined as a PS when the phase of at least two of these three circles was gradually monotonically increasing or decreasing.

In order to track the PSs, we connected PSs at consecutive time instants if their distance was less than 0.1·Y. Finally, we discarded short lasting PSs that did not complete one rotation.

We will show for each measured trajectory the length of the longest diagonal (LD) and its perpendicular (PD).

3. Results

Figure 2 shows the behavior of the clockwise AFL rotating around TA and completing a rotation in 200 ms. The behavior observed is consistent with the literature [1], since the reentrant circuit goes through the cavotricuspid isthmus with a slow conduction velocity allowing recovery of the rest of atrial tissue. Similarly atypical AFL around IVC and SVC was achieved with similar behavior.

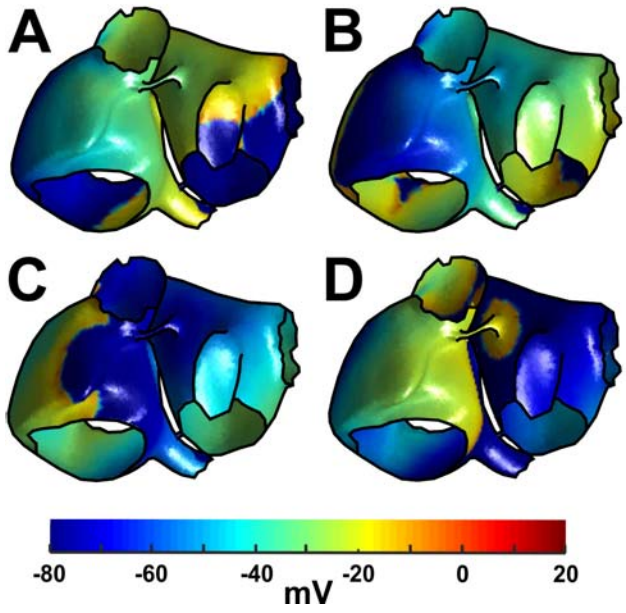

Figure 2: Atrial activation sequence in clockwise typical AFL. Transmembrane potentials at four time instants are shown, representative of a whole period.

Figure 3 shows the phase maps for the four atrial behaviors simulated: sinus rhythm, clockwise AFL, and the atypical flutters around IVC and SVC.

Figure 3.A shows the propagation on the torso during sinus rhythm. Propagation travels from the right shoulder to the left leg which is consistent to previous reports [15].

The propagation during typical AFL is depicted in Figure 3.B. It shows an ascending propagation in the front of the torso continued by a descending propagation in the back according to the previous studies [6]. Two stable PS were detected in the underarms with diagonal lengths (0.16Y, 0.12Y) for the left one and (0.3Y, 0.22Y) for the right one, being Y the height of the torso.

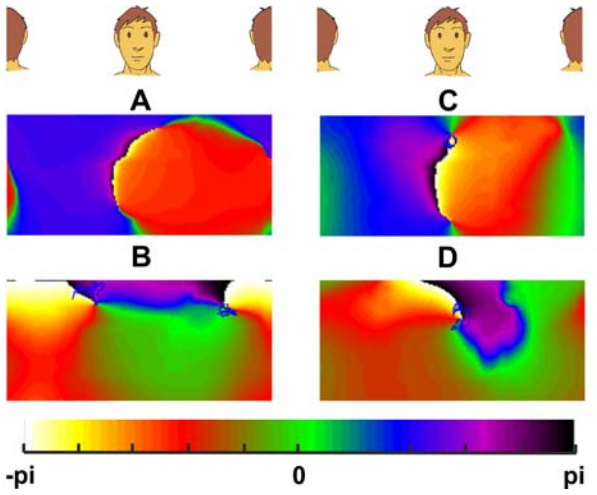

Figure 3: Calculated phase maps and PS tracking (depicted in blue) during sinus rhythm (A), clockwise typical AFL (B) and atypical AFL around IVC (C) and SVC (D).

Figure 3.C and Figure 3.D show phase maps and PS detections during a macroreentrant arrhythmia around the IVC and the SVC respectively. In both cases a counterclockwise propagation in the anterior part of the torso can be observed. The PS detected remained in the front of the torso with diagonal lengths (0.12Y, 0.11Y) for IVC and (0.25Y, 0.16Y) for SVC.

4. Discussion and conclusion

In this study, mathematical models have been used as a tool to characterize the electrocardiographic response during typical and atypical flutters. It has been shown as by using the simulation of atria models and the forward problem we can achieve BSPM recordings very similar to those obtained in clinical practice. This can be used as a tool for the validation when solving the inverse problem of electrocardiography and for the development of new diagnostic tools based in BSPM.

In the present work we also present the phase maps as a tool for interpreting propagation maps in BSPM. This technique facilitates the interpretation of the records obtained as it is able to summarize the direction of

propagation of the signals without performing activation detection and isochronous maps which are highly susceptible to noise. This is due to the capacity of phase maps to summarize the spatial and temporal information in a single image. PS is used to indentify re-entrant patterns in the atrial wall during ex-vivo experiments, in this work we use this technique to summarize the re-entries in the torso model.

As can be observed in our results this technique helped to summarize the BSPM recordings according to the literature [6, 7, 15]. Specifically in the case of sinus rhythm Figure 3.A described a propagation from the right shoulder to the left leg. The typical AFL (Figure 3.B) an ascending propagation through the front of the torso and downward in the back. In the case of atypical flutter, a clockwise propagation around IVC and SVC describes a counterclockwise propagation through the front of the torso. We hypothesize that phase maps and location of the PSs will serve as a technique for the diagnosis, since as we have seen the location and shape of the singularities depends on the obstacle around which AFl is maintained, however, we will require simultaneous recordings of intracardiac and BSPM signals to assess the obtained results.

Despite these limitations, the results of this study reinforce BSPM reliability as a tool for discriminating between different cardiac behaviours, this technique may help in planning ablation procedures in the near future. In addition, the methodology presented defines the feasibility of using modeling as a useful tool in verifying diagnostic techniques based on BSPM and it can be used to clarify the relation between epicardial propagation patterns and its representation on the torso.

Acknowledgements

This work was partially supported by Spanish Ministry of Education (FPU AP2010-4365), Universitat Politècnica de València (PAID-05-12, SP20120483, PAID-2009-2012) and Generalitat Valenciana (GV/2012/039).

References

[1] Garcia-Cosio F, Pastor Fuentes A, Nunez Angulo A. Clinical approach to atrial tachycardia and atrial flutter from an understanding of the mechanisms. electrophysiology based on anatomy. Rev Esp Cardiol 2012; 65:363-75.

[2] Saoudi N, Cosio F, Waldo A, Chen S, Iesaka Y, Lesh M, Saksena S, Salerno J, Schoels W. A classification of atrial flutter and regular atrial tachycardia according to electrophysiological mechanisms and anatomical bases - A statement from a Joint Expert Group from the Working Group of Arrhythmias of the European Society of Cardiology and the North American Society of Pacing and electrophysiology. Eur Heart J 2001; 22:1162-82.

[3] Morady F. Drug therapy - Radio-frequency ablation as treatment for cardiac arrhythmias. N Engl J Med 1999; 340:534-44.

[4] Dubuc M, Nadeau R, Tremblay G, Kus T, Molin F, Savard P. Pace mapping using body-surface potential maps to guide catheter ablation of accessory pathways in patients with Wolff-Parkinson-White syndrome. Circulation 1993; 87:135-43.

[5] Guillem MS, Climent AM, Castells F, Husser D, Millet J, Arya A, Piorkowski C, Bollmann A. Noninvasive mapping of human atrial fibrillation. J Cardiovasc Electrophysiol 2009; 20:507-13.

[6] Guillem MS, Quesada A, Donis V, Climent AM, Mihi N, Millet J, Castells F. Surface wavefront propagation maps: non-invasive characterization of atrial flutter circuit. International Journal of Bioelectromagnetism 2009; 11:22-26.

[7] SippensGroenewegen A, Lesh M, Roithinger F, Ellis W, Steiner P, Saxon L, Lee R, Scheinman M. Body surface mapping of counterclockwise and clockwise typical atrial flutter: A comparative analysis with endocardial activation sequence mapping. J Am Coll Cardiol 2000; 35:1276-87.

[8] Harrild DM, Henriquez CS. A computer model of normal conduction in the human atria. Circ Res 2000; 87:E25-36.

[9] Courtemanche M, Ramirez RJ, Nattel S. Ionic mechanisms underlying human atrial action potential properties: Insights from a mathematical model. Am J Physiol -Heart Circul Physiol 1998; 275(1):H301-21.

[10] Kneller J, Zou RQ, Vigmond EJ, Wang ZG, Leon LJ, Nattel S. Cholinergic atrial fibrillation in a computer model of a two-dimensional sheet of canine atrial cells with realistic ionic properties. Circ Res 2002; 90:E73-87.

[11] Garcia VM, Liberos A, Climent AM, Vidal A, Millet J, Gonzalez A. An adaptative step size GPU ODE solver for simulating the electric cardiac activity. Computing in Cardiology 2011;38; 233-6.

[12] Stenroos M. The transfer matrix for epicardial potential in a piece-wise homogeneous thorax model: the boundary element formulation. Phys Med Biol 2009; 54.

[13] Horacek B, Clements J. The inverse problem of electrocardiography: A solution in terms of single- and double-layer sources on the epicardial surface. Math Biosci 1997; 144:119-54.

[14] Demunck JA. Linear Discretization of the volume conductor boundary integral-equation using analytically integrated elements. IEEE Trans Biomed Eng 1992; 39: 986-90.

[15] Lian J, Li G, Cheng J, Avitall B, He B. Body surface Laplacian mapping of atrial depolarization in healthy human subjects. Med Biol Eng Comput 2002; 40:650-59.

Address for correspondence.

Alejandro Liberos Mascarell
Universitat Politècnica de València. Ed. 8G. Bio-ITACA
Camino de Vera s/n. CP: 46022. Valencia, Valencia, Spain
allimas@upvnet.upv.es